ORIGINAL ARTICLE

Galileo and GLONASS group delay variations

Susanne Beer[1] · Lambert Wanninger[1] · Anja Heßelbarth[1]

Abstract

Similar to the antenna phase center corrections for phase measurements, group delay variations (GDV) of satellite and receiving GNSS antennas affect code pseudorange measurements. They are frequency-dependent and vary with the direction of signal transmission and reception. We present the first GDV estimates for all five Galileo and three GLONASS frequency bands based on terrestrial observations. As compared to GPS, the orbit properties of Galileo and GLONASS simplify this approach, because a single reference station can observe each Galileo and GLONASS satellite in its entire elevation angle range during one orbit repeat period. The homogenous results of three receiver antenna models for identical satellite types and a comparison to GPS Block IIF indicate mainly receiver antenna-specific GDV. They amount to 35 and 28 cm peak-to-peak for Galileo and GLONASS frequency bands E1 and G1, respectively, depending on the receiver antenna type. We show their effect on linear combinations where the code observable is used for precise applications and validate our GDV estimations by improving the height component in single-frequency precise point positioning.

Keywords Galileo · GLONASS · Group delay variations · Code-minus-carrier combination · Multipath combination

Introduction

The code observables of global navigation satellite systems (GNSS) are affected by signal- and frequency-dependent delays. Delays caused by the nonsimultaneous transmission and/or reception of signals result in interfrequency and intersignal biases. They can be corrected by timing group delays and intersignal corrections broadcast in the navigation messages, see, for example, IS-GPS-200 (2018), or by differential code biases estimated by the International GNSS Service (IGS; Montenbruck et al. 2014). Aside from these biases, the code observables show group delay variations (GDV), which vary with the directions of signal transmission at the satellite antenna and signal reception at the receiving antenna.

GDV estimates can be obtained by different methods: Haines et al. (2015) analyzed post-fit residuals from the precise orbit determination (POD) of the two Gravity Recovery and Climate Experiment (GRACE) satellites, Zehentner (2016) estimated GDV for the POD of several low earth orbiting (LEO) satellites based on the raw observation approach, and Wanninger et al. (2017) analyzed the so-called code-minus-carrier linear combination (CMC) of terrestrial observations to determine satellite and receiver antenna corrections.

For GPS, the combined satellite and receiver antenna GDV reach some decimeters in the frequency bands L1 and L2 and 1 m in their ionospheric-free linear combination (IF) depending on satellite block and receiver antenna type (Haines et al. 2015; Zehentner 2016; Wanninger et al. 2017). The published values agree on the level of 10 cm RMS for IF (Beer and Wanninger 2018). They improve precise applications of the code observable, like single-frequency precise point positioning (PPP), ambiguity-fixing with the Hatch–Melbourne–Wübbena linear combination, and the determination of total electron content.

In the case of the Chinese GNSS BeiDou, the BeiDou-2 satellite antennas exhibit GDV much larger than those of GPS (Hauschild et al. 2012a). They are more pronounced for medium earth orbit (MEO) satellites than for inclined geosynchronous orbit (IGSO) satellites and reach up to 1.5 m for frequency band B1. The satellite-induced BeiDou-2 GDV have been studied based on the CMC approach by several groups and can be estimated and corrected (Wanninger and Beer 2015; Yang et al. 2016; Guo et al. 2016; Zou et al. 2017). By analyzing the observations of the first

✉ Susanne Beer
  susanne.beer@tu-dresden.de

1   Geodätisches Institut, Technische Universität Dresden, 01062 Dresden, Germany

experimental BeiDou-3 satellites, Zhou et al. (2018) showed that GDV of this BeiDou satellite generation are much smaller. They are comparable in size to those of GPS Block IIR-M or IIF satellites.

Since individual satellite antenna elements are arranged in circles, their GDV are expected to be mainly nadir-dependent (Okerson et al. 2016). This could be confirmed for GPS by Zehentner (2016) where variations with azimuth occur for only a few satellites and are below 10 cm for single frequencies. Kersten and Schön (2017) determined absolute GDV, which they call code phase variations, for receiver antennas with their robotic device. Significant azimuth dependencies were found for three simple single-frequency antennas but not for the three geodetic-grade antennas they tested.

Whereas GDV of GPS and BeiDou have already been studied (e.g., Wanninger and Beer 2015; Wanninger et al. 2017), GDV of Galileo and GLONASS have not been published until now. Again, we use the CMC approach applied to terrestrial observations to estimate them, because current LEO missions do not provide Galileo and GLONASS observations. No POD is required, but only observation data in the entire elevation range from horizon to zenith for every satellite. For a single satellite, terrestrial stations provide observations in the entire elevation range only if they are located on the satellite's ground track. While GPS ground tracks repeat every (sidereal) day and do not change, the ones of Galileo and GLONASS satellites repeat only after several days and are different in between, see Fig. 1. Thus, their ground tracks produce much denser coverages of the earth's surface than those of GPS. Therefore, a single terrestrial station can observe only a subset of the GPS satellites in their entire elevation range and a set of globally distributed stations is necessary to collect the required observations. In the case of Galileo and GLONASS, however, every single terrestrial station observes all Galileo and GLONASS satellites in their entire elevation range. Because of the advantageous orbit properties, we expect that Galileo and GLONASS GDV can be estimated with the CMC approach at least on the same level of accuracy as in the case of GPS, i.e., 10 cm RMS for IF.

The following section describes the method of estimating GDV with CMC data processing. After presenting the selected data sets, we show the results for Galileo and GLONASS GDV and discuss them in comparison to GPS. Furthermore, the impact of the obtained GDV on linear combinations and the validation of our results are shown. Finally, we summarize the major findings.

Note that the term nadir angle is used synonymously with boresight angle. The satellites are identified by their space vehicle numbers.

Method

GDV are estimated as a function of the nadir angle η at the satellite antenna or the elevation angle e at the receiver antenna. These angles are related by
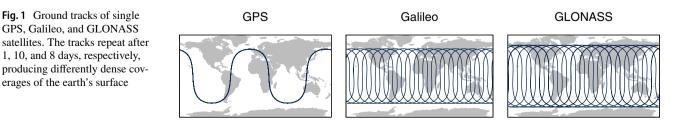
$$\sin \eta = \frac{R}{A} \cdot \cos e \tag{1}$$

where R is the earth's radius and A the geocentric distance of the satellite (Rothacher 2001). For the circular orbits of Galileo and GLONASS, the term R/A is a constellation-specific constant. Maximum nadir angles for observations on the earth's surface are 12.4° and 14.5° for Galileo and GLONASS, respectively.

The combined GDV of satellite and receiver antenna is contained in the code-minus-carrier observable (CMC) which is also known as the multipath combination (MP):

$$\mathrm{CMC}_i = C_i - \phi_i + 2\lambda_i^2 \frac{\Phi_j - \Phi_i}{\lambda_j^2 - \lambda_i^2} - B_i \tag{2}$$

with code pseudorange C, carrier phase Φ, and wavelength λ at frequencies i and j in units of meters (Rocken and Meertens 1992; Hauschild 2017). The contributions of transmitting and receiving antenna cannot be separated since no absolute values are known for either of them. CMC is geometry-, ionospheric-, and tropospheric-free. CMC contains phase ambiguities and biases between the observables caused by hardware and software-induced delays. These biases are lumped together in B_i which is considered constant in continuous ambiguity sequences. Since we process many CMC sequences, we take the various offsets B_i into account and apply an overall zero-mean condition. Therefore, no absolute group delay values can be obtained but only group delay variations.

Fig. 1 Ground tracks of single GPS, Galileo, and GLONASS satellites. The tracks repeat after 1, 10, and 8 days, respectively, producing differently dense coverages of the earth's surface
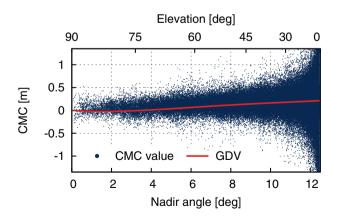
To estimate GDV on centimeter-level, we correct all carrier phase observations for the phase wind-up effect due to satellite rotations (Wu et al. 1993) and apply antenna phase center corrections published by the IGS (Dow et al. 2009). For the receiving antennas, frequency-specific values exist for GPS L1, L2 and GLONASS G1, G2 which we also use for the adjacent Galileo frequencies and GLONASS G3. Concerning the satellite antennas, frequency-specific phase center corrections are available for all five Galileo frequencies. But only ionospheric-free antenna phase center corrections exist for the GLONASS satellites. Even though these values are not intended for individual GLONASS frequencies, we still decided to apply them. We used the geometric distances given by the International Laser Ranging Service (ILRS 2014) between the satellite's center of mass and the GLONASS navigation antenna as a rough clue for the position of the real antenna phase center for single-frequency observations. The geometric distances mostly do not differ from the ionospheric-free values by more than 0.5 m, and thus, their impact on our estimated GDV is small enough (Wanninger et al. 2017).

Figure 2 shows that CMC is dominated by high-frequency code multipath and noise, which is most pronounced for low elevations corresponding to high nadir angles. After applying all corrections, we estimate polynomials of degree four to extract the low-frequency GDV. An elevation-dependent weighting scheme is applied, and the resulting curves are fixed to zero either at zero degrees nadir angle or at a 90° elevation angle. By applying phase center corrections to the phase observables, all estimated GDV refer to the satellite's center of mass and the receiver antenna's reference point. We do not extract code phase center offsets from the nadir or elevation-dependent GDV.

Data

Figure 3 shows the three sets of terrestrial reference stations we chose for our analysis. As outlined above, no globally distributed stations are necessary. Since receiver multipath mitigation techniques can affect pseudorange variations and biases (Hauschild et al. 2012b; Hauschild and Montenbruck 2015, 2016), we selected terrestrial reference stations which use one specific receiver model (SEPT POLARX5). Three subsets with different geodetic-grade antenna models (JAVRINGANT_DM, LEIAR25.R3, and TRM59800.00) allow receiver antenna-specific investigations. Even if a single terrestrial reference station can observe each Galileo and GLONASS satellite in the entire elevation angle range, we aimed for at least ten stations in each subset to reduce site-specific multipath. Therefore, we had to allow mixed receiver firmware versions and station antennas with and without domes. However, in the case of the JAVRINGANT_DM antenna, we could only manage to find four reference stations fulfilling the following requirements: data availability of at least 99%, elevation mask set to 5 degrees or below, and site-specific multipath below 0.5 m RMS for Galileo E1 between 10° and 90°.

Induced by the physical construction of an antenna, the GDV are considered time-invariant, which was confirmed for GPS during a period of more than 2 years by Beer and Wanninger (2018). Therefore, we used observation data of just one orbit repetition period of 10 days (Galileo) and 8 days (GLONASS) from the beginning of 2019. Although each station provides observations in the entire elevation range, the typical distribution shows the most observations in high nadir angles and few observations in nadir direction.

Fig. 2 High-frequency CMC values of twelve terrestrial reference stations and 10 days of observation data for Galileo satellite E211. The low-frequency GDV are estimated by a polynomial of degree four
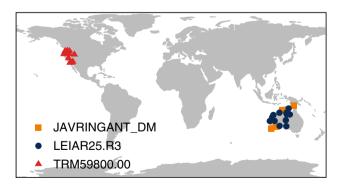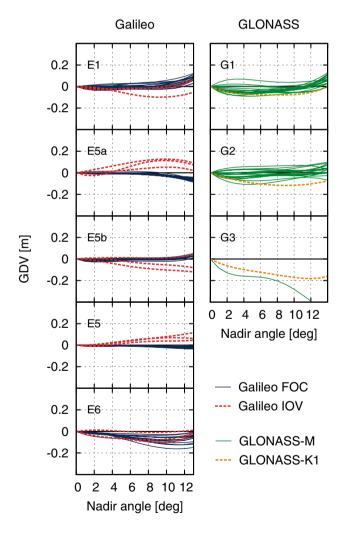

Fig. 3 Three sets of terrestrial reference stations from the networks of UNAVCO and Geoscience Australia, all of them equipped with a SEPT POLARX5 receiver. Yellow squares, blue dots, and red triangles indicate 4, 12, and again 12 stations with JAVRINGANT_DM, LEIAR25.R3, and TRM59800.00 antennas, respectively
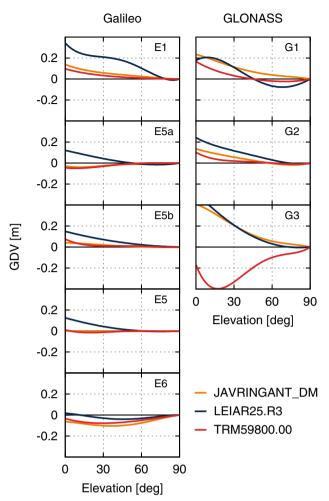
GDV for Galileo and GLONASS

In a first step, we estimated nadir angle-dependent GDV for each satellite in order to detect satellite-individual characteristics. The results for Galileo comprise 17 full operational capability satellites (FOCs) and three in-orbit validation satellites (IOVs). The two Galileo satellites in eccentric orbits are not included. For GLONASS, we obtained results for 19 GLONASS-M and one GLONASS-K1 satellites. Four GLONASS satellites are not included because of an insufficient number of dual-frequency observations.

Figure 4 exemplarily shows the results obtained from the stations equipped with TRM59800.00 antennas. For all three antenna types, Galileo FOCs show homogenous curves with standard deviations smaller 5 cm, while the GDV of IOVs show larger variations. This can be explained by the smaller

Fig. 4 GDV for each Galileo and GLONASS satellite using the example of stations equipped with a TRM59800.00 antenna. Different colors indicate different satellite types, i.e., Galileo FOC and IOV satellites, and GLONASS-M and GLONASS-K1 satellites
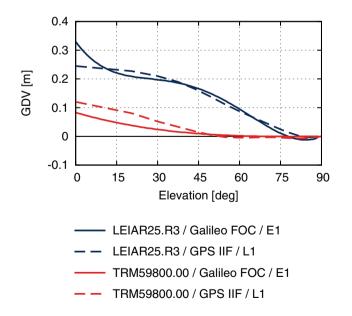
Fig. 5 Receiver antenna-specific GDV for the entire Galileo FOC and GLONASS-M constellations for three receiver antenna types as a function of elevation angle

transmit power of the IOVs leading to a smaller carrier-to-noise ratio (Tian et al. 2019) and affecting the accuracy of GDV estimation. All three receiver antenna types show homogenous GDV for GLONASS-M satellites with standard deviations below 8 cm. The one GLONASS-K1 satellite R802 matches the GLONASS-M satellites in the case of frequency band G1, but differs from the GLONASS-M satellites in the case of G2. Observations in frequency band G3 were available from the GLONASS-K1 satellite R802 and the GLONASS-M satellite R855. The G3 GDV differ from each other and are up to 10 cm peak-to-peak larger than those of G1 and G2.

As described by Arenas et al. (2011), the Galileo IOV satellites exhibited GDV of just 4–12 cm in the individual frequency bands over their entire antenna coverage during tests. It was intended to improve even the GDV performance of the FOC satellites. Since all three antennas show very homogenous results for the FOCs, any differences between

receiver antenna types are attributed to them. Figure 5 shows a comparison of the three receiver antenna models with re-estimated elevation-dependent GDV models for the entire Galileo FOC and GLONASS-M constellation. Concerning Galileo, JAVRINGANT_DM and TRM59800.00 antennas show consistent results. Here, the GDV are most pronounced for frequency bands E1 and E6, but stay below 15 cm peak-to-peak. The LEIAR25.R3 antenna shows larger GDV confirming earlier findings (Wanninger et al. 2017). They sometimes differ in their slope from the other two antennas, especially for frequency band E5a, and reach up to 35 cm peak-to-peak for frequency band E1. In the case of GLONASS and frequency band G1, the GDV amount to 23, 28, and 19 cm peak-to-peak for the JAVRINGANT_DM, LEIAR25.R3, and TRM59800.00 antennas, respectively. Corresponding values for G2 are slightly smaller. Only one GLONASS-M satellite contributes to the results for frequency band G3. Again, the LEIAR25.R3 antenna type shows the largest variations, i.e., 50 cm peak-to-peak, and the GDV of the other two antenna types are slightly smaller, i.e., 40 cm peak-to-peak. However, in contrast to the other results, the curves of the JAVRINGANT_DM and TRM59800.00 antenna types are not similar here.

Galileo has two frequencies in common with GPS: E1 (L1) and E5a (L5). Satellite-individual GDV for GPS L1 were determined by Wanninger et al. (2017) together with several receiver antenna type GDV, among them two of the antenna types investigated here. In Fig. 6, we treat all GDV obtained from GPS Block IIF satellites as purely

receiver antenna-specific by summing up the satellite and the receiver antenna GDV contributions as given in Wanninger et al. (2017) and compare them to the ones obtained from Galileo FOC observations. The good agreement on the level of some centimeters for both antenna types proves that GPS L1 and Galileo E1 GDV are very similar.
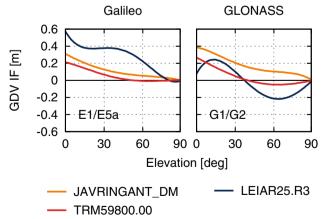
Impact of GDV on linear combinations

The impact of GDV can increase in linear combinations. The following linear combinations are described, for example, by Hauschild (2017). The ionospheric-free linear combination (IF) of two code observables C is formed by

$$\text{IF} = \frac{f_i^2}{f_i^2 - f_j^2} C_i - \frac{f_j^2}{f_i^2 - f_j^2} C_j \tag{3}$$

with f denoting frequencies i and j. Figure 7 shows IF GDV obtained by the combination of Galileo frequencies E1, E5, and GLONASS G1, G2. In the case of Galileo, IF GDV are most pronounced for the LEIAR25.R3 antenna with 0.6 m peak-to-peak while barely half of that for the other two antennas. In the case of GLONASS, the peak-to-peak variations are around 0.4 m for all three antennas. However, the curve shape of the LEIAR25.R3 antenna differs significantly from the other two.

In precise point positioning (PPP), the Hatch–Melbourne–Wübbena linear combination (HMW; Hatch 1982; Melbourne 1985; Wübbena 1985) is used to fix widelane ambiguities. The HMW is the difference of widelane carrier phase observations Φ_{WL} and narrowlane pseudorange observations C_{NL}:

Fig. 6 Comparison of GDV obtained from observations of GPS Block IIF (Wanninger et al. 2017) and Galileo FOC satellites for the frequency band L1/E1 (from upper left panel of Fig. 5) and two different receiver antenna types

Fig. 7 Impact of GDV on the ionospheric-free linear combination (IF) of Galileo frequencies E1, E5a and GLONASS frequencies G1, G2 for three receiver antenna models

$$HMW = \Phi_{WL} - C_{NL} \qquad (4)$$

with

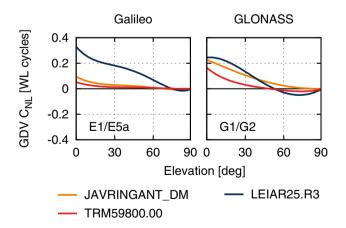$$\Phi_{WL} = \frac{f_i}{f_i - f_j}\Phi_i - \frac{f_j}{f_i - f_j}\Phi_j \qquad (5)$$

$$C_{NL} = \frac{f_i}{f_i + f_j}C_i + \frac{f_j}{f_i + f_j}C_j \qquad (6)$$

where C_i and C_j are the code observables and Φ_i and Φ_j are the phase observables at frequencies f_i and f_j. C_{NL} (6) can be used to demonstrate the effect of GDV on HMW, see Fig. 8. For Galileo E1/E5a, GDV result in less than 0.1 WL cycles peak-to-peak for the JAVRINGANT_DM and the TRM59800.00 antennas, but amount to more than 0.3 WL cycles for LEIAR25.R3. In the case of GLONASS G1/G2, GDV cause variations of around 0.2 WL cycles for the JAVRINGANT_DM and TRM59800.00 antennas and slightly more for the LEIAR25.R3.
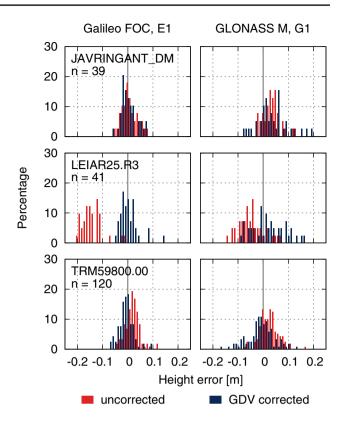
For single-frequency PPP, the GRAPHIC (group and phase ionospheric-free calibration) linear combination is used to eliminate first-order ionospheric effects. It averages code observable C_i and phase observable Φ_i on the same frequency i and thereby reduces the impact of GDV by half:

$$GRAPHIC_i = \frac{C_i + \Phi_i}{2}. \qquad (7)$$

In Fig. 9, we compare PPP results obtained from the uncorrected and GDV-corrected GRAPHIC linear combination for Galileo frequency E1 and GLONASS frequency G1. A multi-GNSS dual-frequency phase solution serves as a reference. One day of observations from IGS, UNAVCO and Geoscience Australia stations equipped with one of the

Fig. 9 Distributions of height errors obtained from single-frequency PPP with the GRAPHIC linear combination. For the corrected solution, GDV from Fig. 5 were applied to Galileo FOC (E1) and GLONASS-M (G1) observations. For the three antenna types (JAVRINGANT_DM, LEIAR25.R3, and TRM59800.00), one day of observations (DOY 005, 2019) of 39, 41, and 120 reference stations were processed

three receiver antenna types of this study were processed. Since elevation-dependent corrections mainly affect the height component, horizontal coordinate errors are not shown here. In the case of the LEIAR25.R3 antenna, the strong elevation-dependent GDV cause systematic height errors of around 12 and 5 cm for Galileo E1 and GLONASS G1, respectively. They are significantly reduced by correcting GDV. In the case of the other two antennas, the GDV cause only small systematic height errors, but still, the corrections improve the height results.

Summary and conclusion

We determined the first group delay variation (GDV) estimates for Galileo and GLONASS based on terrestrial observations and the code-minus-carrier (CMC) linear combination. Because of orbit repeat periods of several days, a single terrestrial reference station can provide Galileo and GLONASS observations from the horizon up to zenith, and no globally distributed network is necessary

Fig. 8 Impact of GDV on code narrowlane (C_{NL}) in widelane (WL) cycles, and thus, on the Hatch–Melbourne–Wübbena linear combination, for Galileo and GLONASS and three receiver antenna types

for the determination of GDV as it is in the case of GPS. However, in order to reduce site-specific multipath, we estimated GDV for three sets of four to twelve reference stations equipped with JAVRINGANT_DM, LEIAR25.R3, and TRM59800.00 antennas.

Individual satellites of the same type show similar GDV. They agree on the level of 5 and 8 cm standard deviation for Galileo FOC and GLONASS-M satellites, respectively. Furthermore, we show that Galileo FOC and GPS Block IIF satellites exhibit very similar GDV.

Receiver antenna-specific GDV are most pronounced for the LEIAR25.R3 antenna type. The GDV of the LEIAR25.R3 antennas amount to 35 cm peak-to-peak for Galileo frequency band E1. Corresponding values for the other two antenna types are around 10 cm. The smallest Galileo GDV of only a few centimeters were determined for frequency band E5 and JAVRINGANT_DM and TRM59800.00 antennas. GLONASS GDV for frequency band G1 amount to 28 cm peak-to-peak for the LEIAR25.R3 antennas and to approximately 20 cm for the other two antenna types. Corresponding G2 GDV are slightly smaller.

The effect of GDV can increase in linear combinations. Ionospheric-free GDV reach up to 0.6 m peak-to-peak, and the contribution of GDV to the Hatch–Melbourne–Wübbena linear combination amounts to 0.3 widelane cycles, each in the case of the most affected LEIAR25.R3 antenna.

Since no Galileo and GLONASS GDV have been published yet, we validate our estimates by applying GDV corrections to single-frequency precise point positioning. Systematic height errors are reduced significantly by up to 12 cm depending on receiver antenna type and frequency band.

GDV estimations for GPS based on the CMC approach using terrestrial observations agreed with the results of other estimation techniques on the level of 10 cm for the ionospheric-free linear combination. Due to the advantageous orbit properties of Galileo and GLONASS, we expect that our GDV estimates reach at least this level of accuracy.

References

Arenas S, Monjas F, Montesano A, Montesano C, Mangenot C, Salghetti L (2011) Performances of GALILEO system navigation antenna for global positioning. In: Proceedings of 5th European conference on antennas propagation, EUCAP. pp 1018–1022

Beer S, Wanninger L (2018) Temporal stability of GPS transmitter group delay variations. Sensors 18:1744. https://doi.org/10.3390/s18061744

Dow JM, Neilan RE, Rizos C (2009) The international GNSS service in a changing landscape of global navigation satellite systems. J Geod 83(3–4):191–198. https://doi.org/10.1007/s00190-008-0300-3

Guo F, Li X, Liu W (2016) Mitigating BeiDou satellite-induced code bias: taking into account the stochastic model of corrections. Sensors 16:909. https://doi.org/10.3390/s16060909

Haines BJ, Bar-Sever YE, Bertiger WI, Desai SD, Harvey N, Sibois AE, Weiss JP (2015) Realizing a terrestrial reference frame using the global positioning system. J Geophys Res Solid Earth 120(8):5911–5939. https://doi.org/10.1002/2015JB012225

Hatch R (1982) The synergism of GPS code and carrier measurements. In: Proceedings of 3rd international geodetic symposium on satellite doppler positioning. Las Cruces, pp 1213–1231

Hauschild A (2017) Combinations of observations. In: Teunissen PJG, Montenbruck O (eds) Springer handbook of global navigation satellite systems. Springer, New York, pp 583–604

Hauschild A, Montenbruck O (2015) The effect of correlator and front-end design on GNSS Pseudorange biases for geodetic receivers. In: Proceedings of ION GNSS+2015, Institute of Navigation, Tampa, pp 2835–2844

Hauschild A, Montenbruck O (2016) A study on the dependency of GNSS pseudorange biases on correlator spacing. GPS Solut 20(2):159–171. https://doi.org/10.1007/s10291-014-0426-0

Hauschild A, Montenbruck O, Sleewaegen J-M, Huisman L, Teunissen PJG (2012a) Characterization of compass M-1 signals. GPS Solut 16(1):117–126. https://doi.org/10.1007/s10291-011-0210-3

Hauschild A, Montenbruck O, Thoelert S, Erker S, Meurer M, Ashjaee J (2012b) A multi-technique approach for characterizing the SVN49 signal anomaly, part 1: receiver tracking and IQ constellation. GPS Solut 16(1):19–28. https://doi.org/10.1007/s10291-011-0203-2

ILRS (2014) SLR Center-of-Mass (CoM) measurement correction information. https://ilrs.cddis.eosdis.nasa.gov/missions/spacecraft_parameters/center_of_mass.html. Accessed 15 Aug 2019

IS-GPS-200 (2018) Global positioning systems directorate, systems engineering and integration, interface specification IS-GPS-200, Revision Journal

Kersten T, Schön S (2017) GPS code phase variations (CPV) for GNSS receiver antennas and their effect on geodetic parameters and ambiguity resolution. J Geod 91:579–596. https://doi.org/10.1007/s00190-016-0984-8

Melbourne WG (1985) The case for ranging in GPS based geodetic systems. In: Proceedings of 1st international symposium on precise positioning with the global positioning system. Rockville, pp 373–386

Montenbruck O, Hauschild A, Steigenberger P (2014) Differential code bias estimation using multi-GNSS observations and global ionosphere maps. Navigation 61:191–201. https://doi.org/10.1002/navi.64

Okerson G, Ross J, Tetewsky A, Soltz A, Anszperger J, Smith SR Jr (2016) Inter-signal correction sensitivity analysis: aperture-dependent delays induced by antenna anisotropy in modernized GPS dual-frequency navigation. Inside GNSS 11(3):44–53

Rocken C, Meertens C (1992) UNAVCO receiver tests. UNAVCO Memo 8

Rothacher M (2001) Comparison of absolute and relative antenna phase center variations. GPS Solut 4(4):55–60. https://doi.org/10.1007/PL00012867

Tian Y, Sui L, Xiao G, Zhao D, Tian Y (2019) Analysis of Galileo/BDS/GPS signals and RTK performance. GPS Solut. https://doi.org/10.1007/s10291-019-0831-5

Wanninger L, Beer S (2015) BeiDou satellite-induced code pseudorange variations: diagnosis and therapy. GPS Solut 19(4):639–648. https://doi.org/10.1007/s10291-014-0423-3

Wanninger L, Sumaya H, Beer S (2017) Group delay variations of GPS transmitting and receiving antennas. J Geod 91(9):1099–1116. https://doi.org/10.1007/s00190-017-1012-3

Wu JT, Wu SC, Hajj GA, Bertiger WI, Lichten SM (1993) Effects of antenna orientation on GPS carrier phase. Manuscr Geod 18(2):91–98

Wübbena G (1985) Software developments for geodetic positioning with GPS using TI 4100 code and carrier measurements. In: Proceedings of 1st international symposium on precise positioning with the global positioning system. Rockville, pp 403–412

Yang W, Tong H, Pan L, Xu D, Guo W, Yang J (2016) Analysis and correction of BDS code multipath bias. In: Sun J, Liu J, Fan S, Wang F (eds) China satellite navigation conference (CSNC) 2016 proceedings, vol III. Springer, Singapore, pp 503–513

Zehentner N (2016) Kinematic orbit positioning applying the raw observation approach to observe time variable gravity. Dissertation, Graz University of Technology

Zhou R, Hu Z, Zhao Q, Li P, Wang W, He C, Cai C, Pan Z (2018) Elevation-dependent pseudorange variation characteristics analysis for the new-generation BeiDou satellite navigation system. GPS Solut 22:60. https://doi.org/10.1007/s10291-018-0726-x

Zou X, Li Z, Li M, Tang W, Deng C, Chen L, Wang C, Shi C (2017) Modeling BDS pseudorange variations and models assessment. GPS Solut 21:1661–1668. https://doi.org/10.1007/s10291-017-0645-2

Susanne Beer is a member of the GNSS research group at the Geodetic Institute of the Technische Universität Dresden (TU Dresden). She received her Dipl.-Ing. degree in geodesy from TU Dresden in 2011. Her research focuses on group delay variations (GDV).

Lambert Wanninger is a professor of geodesy at TU Dresden. He has been involved in research on precise GNSS positioning since 1990. He holds a Dr.-Ing. degree in geodesy from the University of Hannover, Germany, and a habilitation degree in geodesy from TU Dresden.

Anja Heßelbarth is a research associate at TU Dresden. She has been involved in research on precise GNSS positioning since 2005 and holds a Dr.-Ing. degree in geodesy from TU Dresden.